

Evolution of matrix metalloproteinase and tissue inhibitor expression during heart failure progression in the infarcted rat

J. Thomas Peterson*, Hua Li, Lisa Dillon, John W. Bryant

Department of Cardiovascular Therapeutics, Parke-Davis Pharmaceutical Research, Division of Warner-Lambert Company, 2800 Plymouth Road, Ann Arbor, MI 48105, USA

Received 5 October 1999; accepted 18 January 2000

Abstract

Objective: Characterize the timecourse of matrix metalloproteinase (MMP-1, -2, -3, -7, -9, -11, -12, -13, and -14) and endogenous tissue inhibitors of MMPs (TIMP-1, -2, -3, and -4) upregulation during left ventricular (LV) remodeling following myocardial infarction (MI) in rats. **Methods:** The descending left coronary artery of male rats (*Rattus norvegicus*) was ligated to produce a MI. LV function and dilation were assessed from 1 day to 16 weeks post-MI. Protein and mRNA extraction was done on LV samples containing scar and myocardium together. Gelatinase activity was measured by zymography. Westerns were run on the MMPs known to cleave fibrillar collagen in the rat (MMP-8, -13, and -14) as well as TIMP-1, -2, and -4. **Results:** Average infarct size was $38.6 \pm 1.1\%$, and produced LV dysfunction and progressive LV dilation. Thoracic ascites, a marker of congestive heart failure (HF), was not present until 12 weeks post-MI. Upregulation of MMP-2, -8, -9, -13, and -14 and TIMP-1 and TIMP-2 was detected at different timepoints during HF progression. Increased MMP protein levels occurred sometimes without a corresponding elevation in mRNA levels, and increased TIMP mRNA levels without increased protein levels. MMP-13 active form was elevated during the first 2 weeks post-MI while TIMP-1 and TIMP-2 protein levels were not significantly elevated until 2 weeks post-MI. MMP-8 and MMP-14 protein levels increased later during heart failure progression. **Conclusion:** MMP/TIMP upregulation evolves over time following infarction in the rat LV. Some MMPs were significantly elevated during the first week post-MI (MMP-13, -2, and -9) and another was not until 16 weeks post-MI (MMP-14). The dissociation between LV MMP/TIMP mRNA and protein levels shows that post-translation processing occurs in the rat heart. © 2000 Elsevier Science B.V. All rights reserved.

Keywords: Extracellular matrix; Heart failure; Remodeling

1. Introduction

Cardiac fibrosis is a common and well recognized feature of heart failure (HF) [28]. However, collagen accumulation, per se, does not appear to be the only mechanism by which the extracellular matrix contributes to the development of HF. Recent studies indicate that HF may parallel other disease states such as idiopathic pulmonary fibrosis in which maladaptive remodeling involves increased synthesis as well as degradation of extracellular matrix proteins [4,6]. Matrix metalloproteinase (MMP) expression is increased in animals and patients with

systolic heart failure (HF) [2,3,8,13,23,26], and MMPs have a predominant role in extracellular matrix protein turnover [29]. MMP upregulation in the failing heart has been proposed to result in cardiac collagen degradation leading to progressive left ventricular (LV) dilation and pump dysfunction. Corroboration of the role of MMPs in maladaptive ventricular remodeling is available from studies showing that MMP-inhibition reduces LV dilation and preserves LV ejection fraction in animal HF models [19,22]. Increased MMP activity in HF may also occur via the downregulation of the endogenous tissue inhibitors of MMPs (TIMPs) [3,13] and/or to a decrease in the MMP/TIMP complex [3].

The purpose of the present study was to characterize the

*Corresponding author. Tel.: +1-734-622-7189; fax: +1-734-622-1480.

E-mail address: tom.peterson@wl.com (J.T. Peterson)

Time for primary review 30 days.

temporal progression of MMP, TIMP and collagen expression in the myocardial infarct (MI) rat HF model. MMP-1, -2, and -9 and TIMP-1 expression have previously been characterized during the first month post-MI in the rat [2]. The current study assessed the mRNA and/or protein levels of several additional MMPs (-3, -7, -8, -13, and -14) and TIMPs (-2, -3, and -4) out to 4 months post-MI, a point at which some rats develop congestive heart failure. MMP expression has been reported to be transcriptionally mediated [27], therefore, mRNA and protein levels were expected to parallel each other. MMP-1 was assessed because the presence of this enzyme is controversial in rats. MMP-8 (neutrophil collagenase), MMP-13 (type 3, or rat interstitial collagenase), and MMP-14 (membrane-type 1 MMP) were measured because each of these enzymes are recognized to cleave fibrillar collagen [17]. Stromelysin (MMP-3) does not cleave fibrillar collagen, but stromelysin has been shown to activate other MMPs thus potentially contributing to increased collagenolysis [29]. In addition, stromelysin, matrilysin (MMP-7), and the gelatinases (MMP-2 and MMP-9) may contribute to LV remodeling by altering the basement membrane which is important in molecular traffic around cardiocytes, vascular permeability, and LV hydration [1]. Accordingly, the objectives of this study were to determine: whether a specific MMP(s) was upregulated throughout HF; if TIMP downregulation occurred; and does the pattern of MMP/TIMP expression change at timepoints associated with the development of congestive heart failure.

2. Methods

2.1. Experimental design of efficacy experiment

Male 6-week-old Sprague-Dawley rats were infarcted by ligation of the left anterior descending coronary artery using a silk ligature at Charles River, and shipped to Parke-Davis. LV function and dilation was assessed at varying intervals (1, 2, 3, 5, 8, 10, 12, and 16 weeks post-MI) following MI. Assessment of MMP and TIMP expression was assessed on day 1 post-MI using tissue harvested at Charles River. A total of three to eight SHAM and eight to 13 MI-rats were used for each timepoint. All rats were maintained on a 12-h light/dark cycle, and had ad libitum access to food and water. All procedures and protocols involving the use of animals were approved by the Parke-Davis Animal Care and Use Committee, and conformed with the *Guide for the Care and Use of Laboratory Animals* published by the US National Institutes of Health (NIH Publication No. 85-23, revised 1996).

2.2. LV function and geometry

Rats were anesthetized with isoflurane, a tracheotomy performed, and rats respired at 1 l/min with a ventilator

(ADS 1000, Engler Engineering Corp., Hialeah, FL). A pressure transducer (Millar SPR-249 or SPR-612, Houston, TX) was advanced into the LV via the right carotid to measure maximal and minimal value of the first derivative of LV pressure ($+dP/dt$ and $-dP/dt$, respectively), LV end-diastolic pressure (EDP) and end-systolic pressure (ESP), and heart rate (HR). The signal from the Millar was amplified with a transducer amplifier (model 13-4615-50, Gould Instrument Systems, Inc., Valley View, OH), and data was recorded using a digital data acquisition system (Po-Ne-Mah model P3 v 2.02, Gould). Baseline LV function was measured at a fixed LV end-systolic pressure (LVESP) of 120 mmHg to normalize for the effect of differences in afterload. An LVESP of 120 mmHg was obtained by adjusting the amount of isoflurane anesthesia between 1.5 and 1.0%. A 10–30-s average was used for both baseline and low anesthesia measurements of LV performance. A sternotomy was performed, the aortic root isolated, and a 00 silk suture placed around the aorta. Outflow from the aorta was occluded to generate isovolumic beats so that LV peak developed pressure (PDP) could be measured. LV PDP was defined as the difference between LVESP and LVEDP.

After the completion of LV functional measurements hearts were arrested by intravenous administration of 1 cc of a supersaturated solution of KCl. The heart was excised and a glass cannula was inserted into the LV via the aorta. A ligature was securely tied around the atrio-ventricular groove that sealed the LV. The heart was suspended in air beneath the cannula, and cardiac dilation was measured by generating LV pressure-volume (PV) curves. Two or three PV curves were generated by evacuating the LV of saline and then filling the LV at a fixed rate using a programmable pump set at a 1 ml/min flow-rate, and LV pressure recorded using the Po-Ne-Mah digital data acquisition system.

Upon completion of functional measures the heart was taken off the cannula, and the atria and right ventricle (RV) quickly removed. The RV was weighed. A 2–3-mm cross-section of the LV (at the level of the right ventricular papillary muscles) was taken and immersion fixed in buffered 10% formalin. The remainder of the LV tissue was frozen in liquid N₂. Chamber weights were determined by weighing both frozen and fixed LV tissue. All subsequent biochemical analysis of the LV includes scar, border, and remote zones.

The formalin-fixed LV specimens were embedded in molten paraffin, and 5- μ m sections prepared for histology. A Masson's trichrome stained cross-section from each heart was used to assess MI-size in each animal. Slides were digitized on a flatbed color scanner (Relisys 9624) at a resolution of 600 DPI. MI size was quantified by manually tracing the epicardial circumference of the scar and LV. Scar size was expressed as the percentage of the LV free wall and septum that was comprised solely of transmural or endocardial connective tissue. Only rats with an MI-size $\geq 20\%$ were used in this analysis.

2.3. Northern analysis

Total RNA was extracted from frozen LV tissues using guanidinium thiocyanate phenol chloroform (Trizol, Gibco-BRL, Gaithersburg, MD). Total RNA (20 µg) was electrophoresed in 1.2% agarose gels, transferred to a nylon membrane (ZetaBind, Life Science Product Inc., Gaithersburg, MD) with 20× SSC, and fixed by ultraviolet crosslinking. All of the probes were labeled with ³²P-dCTP by random priming method (Amersham, Arlington Heights, IL) and purified by spin column (Boehringer Mannheim, Indianapolis, IN). The pre-hybridization and hybridization were performed at 42°C for 1 and 16 h, respectively, followed by post-hybridization washes at 55°C with 2× SSC in 1% sodium dodecyl sulfate (SDS) for 2×10 min. and 0.1× SSC/1% SDS for 25 min. Autoradiography was performed by exposure to a Kodak film at –80°C for 24–48 h. To control the variations in sample loading, a mouse glyceraldehyde-3-phosphate dehydrogenase (GAPDH) cDNA fragment (Ambion Inc., Austin, TX) was used to normalize all blots. The results are reported as the ratio of the specific probe to the GAPDH.

2.4. Source of cDNA probes

The probes used for this study were MMP-1, a 2.05-kb *HindIII/SmaI* fragment from human MMP-1 cDNA (American Type Culture Collection, MD); MMP-2, a 930-bp *EcoRI/XbaI* fragment from rat MMP-2 cDNA (Dr John Jeffery, Albany Medical College, Albany, NY); MMP-3, a 1.6-kb *EcoRI* fragment from rat stromelysin cDNA (Dr Lynn M. Matrisian, Vanderbilt University, Nashville, TN); MMP-7, a 740-bp *EcoRI* from rat matrilysin cDNA (Dr Susan Abramson, University of Miami, Miami, FL); MMP-9, a ~300-bp *EcoRI/HindIII* fragment which contains exon-13 of mouse gelatinase B gene (Dr Steve Shapiro, Washington University, St. Louis, MO); MMP-13, a mix of 1.2 and 1.4-kb *EcoRI* fragments from rat interstitial collagenase cDNA (Dr John Jeffery, Albany Medical School, Albany, NY); MMP-14, a 400-bp cDNA segment created with rat heart mRNA and the primers GGACCATGTCTCCCGCCCCWGMACCT and TGGGSGTCAGACCTTGTCAGCA (5' to 3') (W=t or a; M=c or a; S=c or g); TIMP-1, a 700-bp *EcoRI* fragment from mouse TIMP-1 cDNA; TIMP-2, a 700-bp *EcoRI* fragment from mouse TIMP-2 cDNA; TIMP-3, a 750-bp *EcoRI* fragment from human TIMP-3 cDNA; and TIMP-4, a 700-bp *EcoRI* fragment from human TIMP-4 cDNA (all TIMP probes provided by Dr Yi Sun, Molecular Biology, Parke-Davis, Ann Arbor, MI).

2.5. Preparation of LV tissue extracts

Protein samples containing MMP activity were extracted from the same set of samples used for RNA analysis. Frozen LV tissues (~50 mg) were homogenized in 1 ml of

ice-cold lysis buffer containing 150 mM NaCl, 20 mM Hepes, 0.2 mM ethylenediaminetetraacetic acid (EDTA), 25% glycerol and protease inhibitor (complete, Boehringer Mannheim). The homogenates were then centrifuged for 10 min at 4°C at 14 000 rpm, and the supernatant was transferred into a clean tube and kept on ice. Protein concentration was determined by using a standard protein assay (Bio-Rad protein assay, Bio-Rad, Richmond, CA). The extracted samples were then aliquoted and stored at –80°C until use.

2.6. Gelatin and casein zymography

Gelatin and casein zymography was also used to determine MMP protein levels as described elsewhere [16]. Cell extracts were thawed on ice, and the volume of 30 µg of protein was adjusted to 10 µl, then mixed with an equal volume of 2× SDS gel sample loading buffer (126 mM Tris-HCl, 20% glycerol, 4% SDS, 0.005% bromophenol blue, pH 6.8), incubated for 10 min at room temperature prior to loading to the gelatin gel (Novex, San Diego, CA). Gels were run at 80 V at room temperature until the dye reached the bottom of the gel, then gels were incubated with renaturing buffer and developing buffer at room temperature for 30 min each, changed to fresh developing buffer once and incubated at 37°C for 24–48 h. Gels were stained with Coomassie Brilliant Blue (0.2%). A separate set of gelatin and casein gels were developed in the presence of 20 mM EDTA to determine whether lytic banding represented MMP specific activity.

2.7. Western blot analysis

LV tissue extracts containing 40 µg total protein were electrophoresed on a 4–20% Tris-glycine gel, and then transferred onto a nitrocellulose filter. After blocking, the filter was incubated with diluted antibody and matched secondary antibody. Protein bands were visualized using an ECL mixture (NEN Life Science Products, Inc., Boston, MA). Blots were stripped, and this process repeated with a second antibody. All antibodies, except MMP-14, were obtained from Chemicon (Temecula, CA). Three sets of blots were prepared. The first set was used to measure TIMP-4 (AB816, 1:1000). The second set was used to measure TIMP-1 (AB800, 1:1000), and TIMP-2 (AB801, 1:1000). The third set was used to measure MMP-8 (AB8115, 1:1000), MMP-13 (MAB3321, 1:2000) and MMP-14 (Oncogene, IM39L, 10 µg/ml).

2.8. Data analysis

An internal control was also used for all zymograms as well as Northern and Western blots to control for between-gel variability. All Northern, Western, and zymograms were scanned by a densitometer, and analyzed by image quantitation software (Molecular Dynamics, Version 4.2a, Sunnyvale, CA). Descriptive statistics are expressed as

group means \pm standard error. Physiological data from all rats was analyzed based on absolute values using a one-way analysis of variance to test for treatment effects, and between groups differences were assessed using a post-hoc *t*-test. Total LV (infarct, border, and remote) RNA from eight representative MI-rats and two control rats from each timepoint were used. Protein samples from six control rats, and six representative MI-rats were used for protein level determinations at 1, 2, 5, 8, and 16 weeks post-MI. Response variables were expressed as the percent change from control and were analyzed using a rank-order one-way analysis of variance. If the ANOVA generated a *P*-value ≤ 0.05 then comparisons were made from each follow-up time interval versus the control group mean using a Dunnett's multiple comparison test (SAS v6.12, SAS Institute Inc.). Statistical significance was based on a *P*-value ≤ 0.05 .

3. Results

The rats tested in this study ranged from 7 to 22 weeks of age, a period of dynamic growth with body and LV weights doubling in Sham control and MI-rats (Table 1). MI-rats had a lower mean body weight throughout the study compared to Shams, however, this result was not statistically significant. There was no difference in LV weights between the Sham and MI-rats at any timepoint. Mean Sham RV weights remained constant across the timeframe of this study. Progressive RV hypertrophy occurred in MI-rats starting at 3 weeks post-MI.

3.1. Physiological changes during heart failure progression

Mean MI-size was $38.6 \pm 1.1\%$ based on LV circumference, and MI-size did not significantly change over time. The LV pressure-volume relations (Fig. 1) show the progressive dilation of MI-rats that occurred during the timeframe of this study. At 16-weeks post-MI LV volume at a fixed pressure of 20 mmHg was 81% greater in

MI-rats compared to age-matched Shams (Table 2). Masson's trichrome stained cross-sections from representative Sham (top) and MI-rats (bottom) at 1, 8, and 16 weeks post-MI (at the bottom of Fig. 1) illustrate LV remodeling over 16 weeks.

Isoflurane anesthesia was adjusted to create an LVESP of 120 mmHg, and there was less than a 4-mmHg difference in LVESP between Sham controls and MI-rats across all timepoints. LVEDP was elevated, $+dP/dt$ and PDP were lower at all time-points, and LV volume at a fixed pressure of 20 mmHg progressively increased in MI-rats compared to Shams (Table 3). None of these variables showed a significant time effect. Congestive heart failure defined as the presence of thoracic ascites was evident starting at 12 weeks post-MI (Table 3). Although cardiovascular function did not appear to alter at 12 and 16 weeks post-MI, MI-rats with ascites lost body weight, had a substantially higher LVEDP, and a significant drop in LV $+dP/dt$ and $-dP/dt$, and PDP (Table 4). Extent of infarction did not differentiate which rats had ascites as MI-size was comparable between groups.

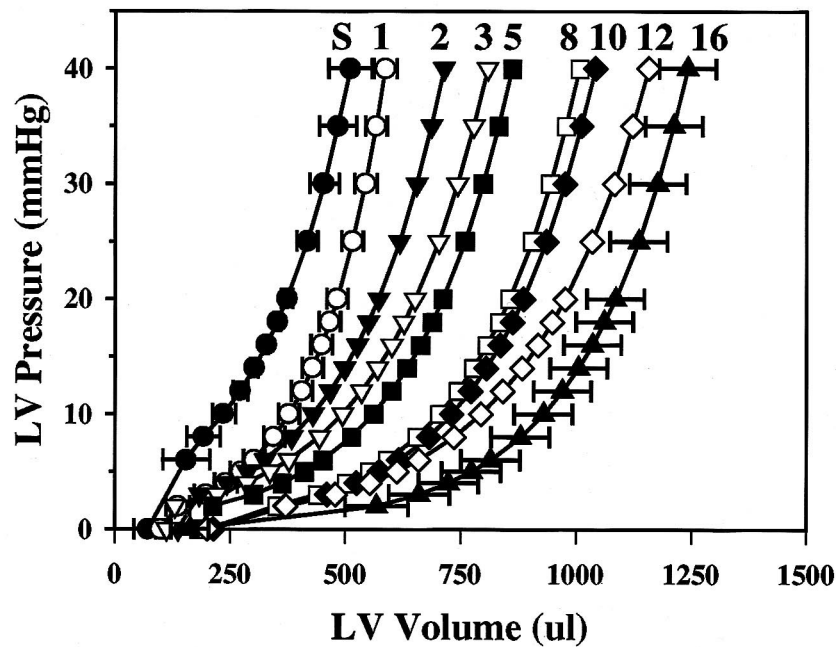
3.2. MMP expression

Both MMP-2 mRNA and protein levels as measured by zymography increased following MI compared to Sham control (Fig. 2, left-panel). MMP-2 mRNA levels were elevated within 24 h post-MI, and peaked around 2 weeks post-MI. MMP-2 mRNA and protein levels paralleled each other during the first 8 weeks post-MI. However, MMP-2 zymographic activity increased again starting at 10 weeks post-MI while mRNA levels remained near baseline. The addition of 20 mM EDTA in the development buffer to a separate group of zymogram gels abolished the lytic bands, and confirmed that gelatin zymogram lytic banding was the result of MMP activity. No EDTA sensitive bands were found on casein gels. MMP-9 protein levels as measured by zymography was elevated from 1 to 16 weeks post-MI (Fig. 2, right-panel). MMP-9 mRNA levels were difficult to measure by Northern in the LV because of low expression levels, and a significant increase was not

Table 1
Absolute change in body weight and cardiac chamber weight over 1–16 weeks post-MI in rats

Weeks post-MI	N		Body weight (g)		LV (mg)		RV (mg)	
	Sham	MI	Sham	MI	Sham	MI	Sham	MI
1	-	12	-	178 \pm 6	-	516 \pm 28	-	128 \pm 8
2	3	12	320 \pm 12	248 \pm 8	631 \pm 16	598 \pm 15	228 \pm 18	255 \pm 22
3	4	10	348 \pm 8	323 \pm 8	734 \pm 77	758 \pm 24	224 \pm 29	306 \pm 34 ^a
5	5	13	381 \pm 15	353 \pm 5	818 \pm 46	818 \pm 29	225 \pm 15	319 \pm 20 ^a
8	5	10	421 \pm 18	390 \pm 14	858 \pm 46	914 \pm 36	250 \pm 17	358 \pm 38 ^a
10	5	8	471 \pm 28	454 \pm 23	890 \pm 18	936 \pm 27	269 \pm 7	366 \pm 36 ^a
12	8	13	512 \pm 16	488 \pm 21	932 \pm 39	975 \pm 35	262 \pm 5	426 \pm 36 ^a
16	6	10	544 \pm 20	503 \pm 16	1005 \pm 41	1011 \pm 36	237 \pm 15	425 \pm 27 ^a

^a *P* ≤ 0.05 compared to Sham.



1-Wk

8-Wk

16-Wk

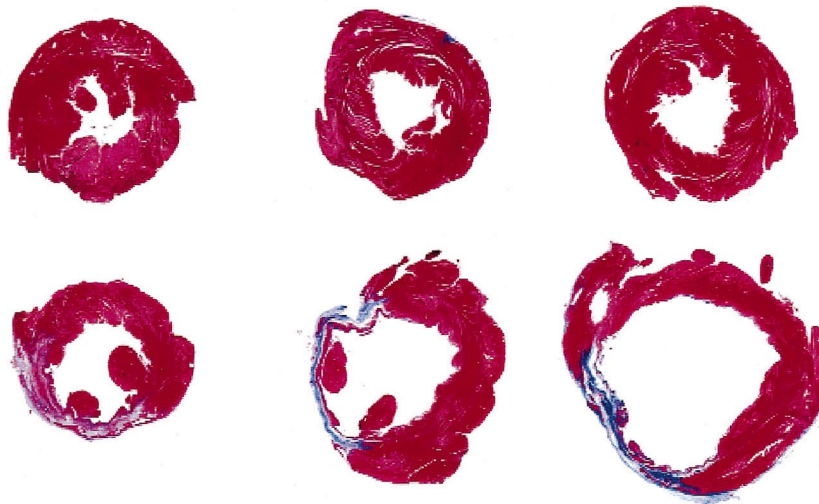


Fig. 1. Left ventricular (LV) pressure volume curves for each time-point tested with the week noted above each curve (top). Data for sham controls between 2 and 16 weeks post-surgery were combined into one curve. Standard error bars are shown for the Sham, 1 week, and 16 week post-MI groups. Representative Masson's trichrome LV cross-sections illustrating progressive LV remodeling at 1, 8, and 16 weeks post-MI.

observed. This result suggests that zymography was more sensitive, and therefore more readily able to detect differences in MMP-9 expression.

Although mean MMP-13 mRNA levels appeared to show an early and late peak (Fig. 3, line-graph), an ANOVA revealed no significant difference. However,

significant changes in MMP-13 protein levels were observed (Fig. 3, bar chart). MMP-13 active form was increased during the first 5 weeks post-MI. A significant decrease in pro-MMP-13 occurred at 1 week post-MI, and protein levels were elevated from 5 to 16 weeks post-MI. The pro-form of both MMP-8 (neutrophil collagenase) and

Table 2
Time-course of hemodynamic changes following myocardial infarction in anesthetized rats

Weeks post-MI	LVEDP (mmHg)		LV +dp/dt (mmHg/s)		PDP (mmHg)		LV Volume (μl)	
	Sham	MI	Sham	MI	Sham	MI	Sham	MI
1	-	13.5±2.8	-	4400±246	-	140±7	-	497±24
2	5.1±1.7	17.7±3.2 ^a	5914±237	4128±177 ^a	186±10	147±6 ^a	383±10	583±21 ^a
3	3.4±1.2	15.7±3.4 ^a	5748±178	4760±296 ^a	189±8	144±6 ^a	575±51	720±34 ^a
5	3.3±1.7	18.0±3.1 ^a	6042±248	4376±132 ^a	184±8	148±5 ^a	527±27	667±46 ^a
8	4.9±1.5	20.2±2.6 ^a	6086±303	4240±244 ^a	190±4	123±6 ^a	538±25	850±39 ^a
10	1.0±0.8	16.7±4.2 ^a	6226±149	4417±201 ^a	188±5	141±10 ^a	573±37	873±56 ^a
12	3.0±1.4	20.1±3.9 ^a	5804±176	4892±208 ^a	208±6	138±7 ^a	560±44	1002±59 ^a
16	3.4±0.6	25.6±4.4 ^a	6362±200	4908±278 ^a	212±7	123±7 ^a	614±54	1114±62 ^a

^a *P*≤0.05 compared to Sham.

Table 3
Incidence of thoracic ascites indicative of congestive heart failure

Weeks post-MI	N size	Thoracic ascites
1	12	0
2	12	0
3	10	0
5	13	0
8	10	0
10	8	0
12	13	4
16	10	3

MMP-14 (membrane type-1 MMP) protein levels were also significantly increased (Fig. 4).

3.3. TIMP expression

TIMP-1 mRNA levels were significantly elevated throughout the study, peaking at 1 day post-MI and steadily diminishing until 5 weeks post-MI (Fig. 5, line-graph). TIMP-1 protein levels did not increase until 2 weeks post-MI, returned to baseline at 3 weeks post-MI, and then did not increase again until the end of the study (Fig. 5, barchart). TIMP-2 mRNA levels were significantly increased during the first 3 weeks post-MI, returned to baseline from 5 to 10 weeks post-MI, and increased again at 12 weeks post-MI (Fig. 6, line-graph). TIMP-2 protein levels also did not show a significant increase until 2 weeks post-MI, and were not significantly increased at 8 weeks post-MI (Fig. 6, barchart). Although TIMP-1

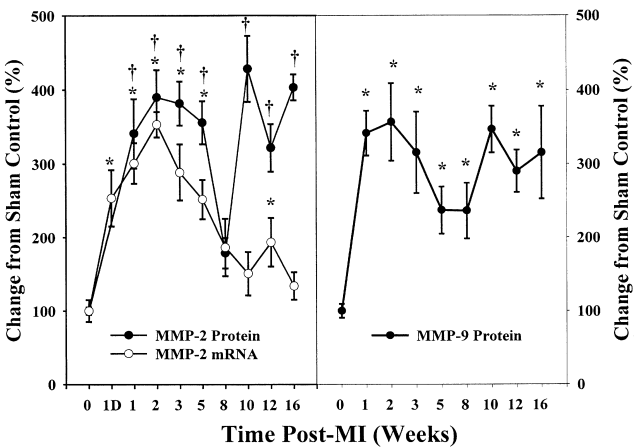


Fig. 2. Percent change in MMP-2 mRNA and zymographic activity in MI-rats compared to Sham controls (left), and MMP-9 zymographic activity (right). Samples from two to three Sham controls at each timepoint were used. Both MMP-2 mRNA and zymographic activity were increased at all timepoints tested until 8 weeks post-MI. After 8 weeks post-MI MMP-2 zymographic activity showed a substantial increase which was not paralleled by increased mRNA levels. MMP-9 was significantly elevated throughout the study. * *P*≤0.05 for MMP-2 mRNA or protein compared to Sham; † *P*≤0.05 for MMP-2 zymographic activity compared to Sham.

mRNA levels were three-fold higher than that of TIMP-2 at 2 weeks post-MI, the increase in protein levels was approximately the same for these two genes. TIMP-4 mRNA levels did not change over time, however, protein levels decreased by more than 50% at 1 and again at 8 weeks post-MI (Fig. 7).

Table 4
Comparison of cardiovascular function of MI-rats with thoracic ascites compared to those without at 12 and 16 weeks post-MI

	MI-Size (% LV)	Body wt (mg)	LVEDP (mmHg)	+dp/dt (mmHg/s)	-dp/dt (mmHg/s)	PDP (mmHg)
No ascites	35±2	513±10	18±3	5161±142	3512±113	140±4
Ascites	38±4	423±30 ^a	38±3 ^a	4044±258 ^a	3036±157 ^a	104±8 ^a

^a *P*≤0.05 compared to MI-rats without thoracic ascites.

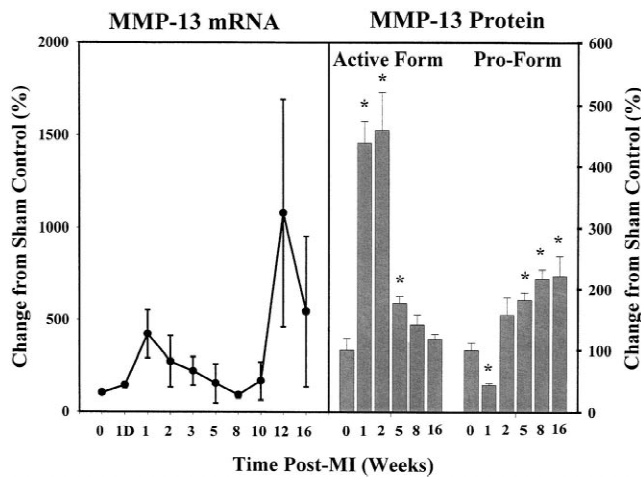


Fig. 3. Percent change from Sham control levels for MMP-13 mRNA (line-graph on left, $N=8$ per timepoint) and protein (barchart on right, $N=6$ per timepoint). Mean changes in MMP-13 mRNA levels were not significant. MMP-13 active form was increased at 1 and 2 weeks post-MI, and pro-MMP-13 was increased starting at 5 weeks post-MI. * $P \leq 0.05$ compared to Sham.

4. Discussion

This study shows that of the a significant increase in the active form of rodent interstitial collagenase (MMP-13) predominates the early post-ischemic period while neutrophil collagenase (MMP-8) and membrane type-1 MMP (MMP-14) increase during later remodeling. In addition, the novel observation was made that MMP protein levels can increase without a change in mRNA levels and TIMP mRNA levels can increase without a change in protein levels. A limitation of the current study is that a regional analysis of gene and protein expression was not performed.

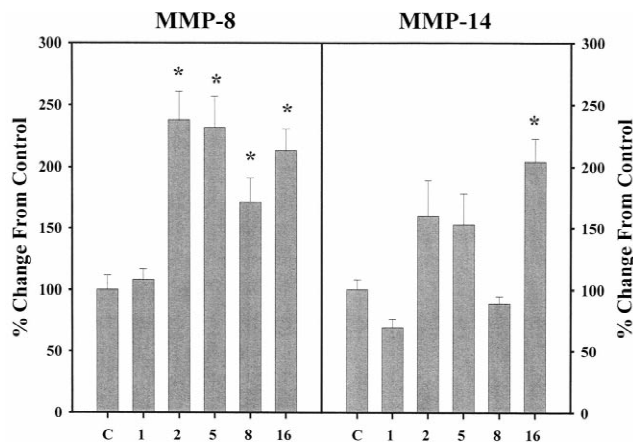


Fig. 4. Percent change in MI-rat MMP-8 (barchart on left, $N=6$ per timepoint) and MMP-14 (barchart on right, $N=6$ per timepoint) protein levels vs. sham control. MMP-8 increased starting at 2 weeks post-MI, and MMP-14 was significantly increased only at 16 weeks post-MI. * $P \leq 0.05$ compared to Sham.

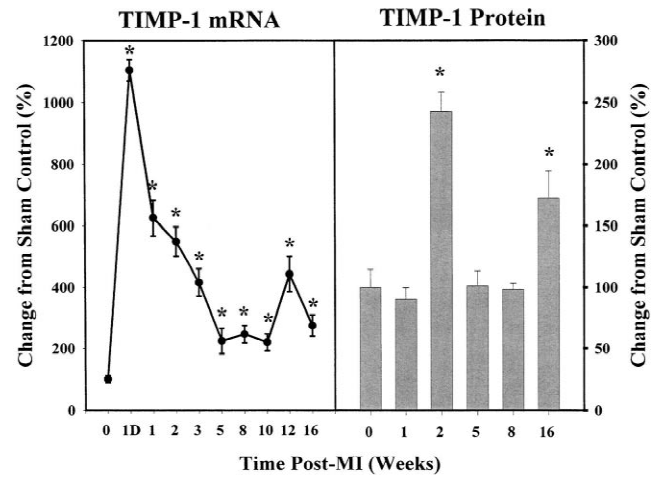


Fig. 5. Percent change in MI-rat TIMP-1 mRNA (line-graph on left, $N=8$ per timepoint) and protein (barchart on right, $N=6$ per timepoint) levels vs. sham control. * $P \leq 0.05$ compared to Sham.

However, Shimizu et al. [21] have recently shown that although MMP-2 shows the greatest elevation in the infarcted region of the rat LV that MMP-2 is also significantly increased in the border zone and remote zones too. Studies showing that the inhibition of MMP activity in both the MI-mouse [9,19] and paced pig [15,22] ameliorate LV dilation support the role of MMPs in ventricular remodeling.

4.1. Temporal progression of MMP upregulation

Although mRNA levels of several MMPs (-2, -3, -7, -9, -11, -13, and -14) were assessed only MMP-2 showed a significant increased in transcriptional activity. However, LV protein levels for several other MMPs (-9, -8, -13, and

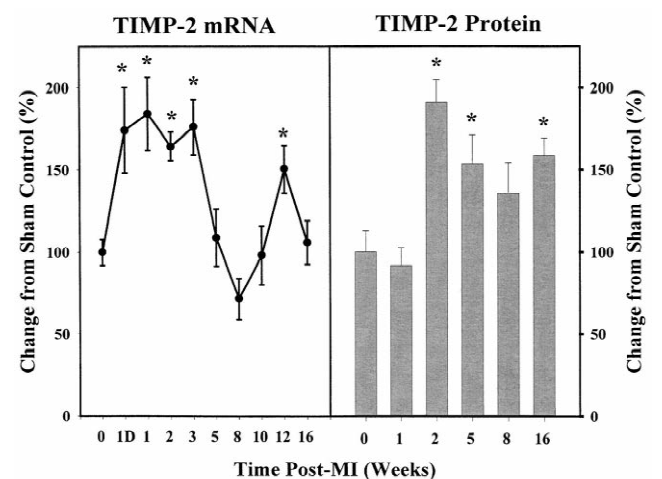


Fig. 6. Percent change in MI-rat TIMP-2 mRNA (line-graph on left, $N=8$ per timepoint) and protein (barchart on right, $N=6$ per timepoint) levels vs. sham control. * $P \leq 0.05$ compared to Sham.

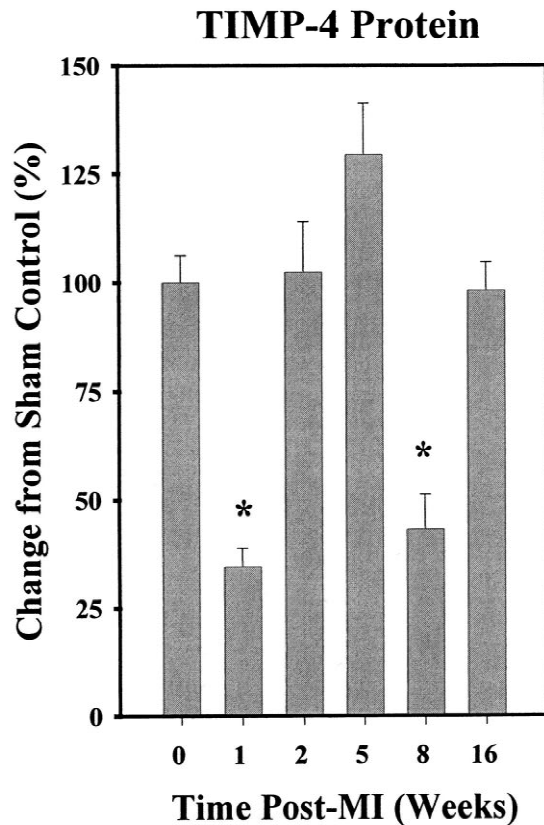


Fig. 7. Percent change in MI-rat TIMP-4 protein levels ($N=6$ per timepoint) levels vs. sham control. * $P \leq 0.05$ compared to Sham.

–14) were increased revealing the importance of MMP protein level determinations in HF. Scar formation is more rapid in the infarcted rat heart (2–3 weeks) compared to larger animals such as the dog [12]. MMP-13 active form, MMP-2, and MMP-9 were elevated throughout this period while MMP-8 levels increased at the end of scar formation. Levels of pro-MMP-13 were reduced at 1-week post-MI compared to sham controls presumably due to increased activation. Free radical-induced MMP activation was used to explain the 50% loss of collagen measured in infarcted rat LV following a 3-h coronary artery ligation [24]. Mice lacking tissue-type plasminogen activator, urokinase receptor, have been shown to have reduced MMP activation and LV dilation following MI [9]. Increased urokinase receptor density and/or activity, and/or increased activity of another serine protease may have also contributed to elevated MMP-13 activation. MMP-14 has been shown to activate MMP-13, but given the lack of change in MMP-14 protein levels until the end of the study it is unlikely it played a role.

Cytokine stimulation does not appear to mediate MMP-2 expression [11]. Increased mechanical stress [5], angiotensin-II induced fibroblast proliferation [25], and increased enzyme stability by extracellular matrix proteins [10] may have contributed to increased MMP-2. MMP-9 upregulation may have occurred in response to cytokines (e.g.

TNF α and IL-1 β) [11], mechanical stress [5], or macrophage infiltration [18]. Increased MMP-8 indicates granulocyte accumulation and/or stimulation. A 30-fold increase in neutrophil collagenase (MMP-8) mRNA levels has been reported in human HF patients [8], however, neutrophils were not observed in histological specimens from the same patients (Dr J.F. Woessner, University of Miami School of Medicine, personal communication). It is unclear what cell type contributed to increased MMP-8, or whether this increase took place within the cardiac interstitium or in inflammatory cell secretory granules.

Cleutjens et al. [2] observed an increase in MMP-2, MMP-9, and TIMP during the first month post-MI in the rat heart. The timecourse of gelatinase upregulation was more rapid in this earlier study. MMP-2 peaked earlier (1 vs. 2 weeks post-MI) and declined faster (2 vs. 8 weeks post-MI), and MMP-9 returned to baseline after 3 weeks post-MI. The reason for this difference is not obvious because the same strain of rat, and mean MI-size were involved in both studies. Cleutjens et al. also reported the presence of MMP-1 in the rat heart by in situ hybridization while no evidence of MMP-1 was found by Northern in this study. However, the probe used in this study reflected MMP-13 hybridization (Dr J.P.M. Cleutjens, University of Limburg, personal communication), and possibly recent reports by others of MMP-1 in the rat heart are due to the same problem [20].

4.2. TIMP expression

TIMPs are expressed by both myocytes as well as non-myocytes within the heart [14]. TIMP-1 and TIMP-2 protein levels increased, and TIMP-4 protein levels decreased at different times within this study. Cleutjens et al. [2] also reported an increase in TIMP-1 mRNA out to 14 days post-MI in rats, and increased TIMP-1 and TIMP-2 protein levels have been reported in the failing human heart [26]. However, another group which studied mRNA and protein levels for all four TIMP isoforms in HF patients reported that TIMP-1, -3, and -4 protein levels decrease while TIMP-2 remains unchanged, and mRNA and protein levels both decreased (except for TIMP-4) [13]. In the current study, elevations in TIMP-1 and TIMP-2 protein levels lagged 2 weeks behind increased mRNA levels showing that post-translation processing of these two TIMP isoforms occurs in the rat heart. TIMP-1 is regulated by cytokines and growth factors [14], and TNF α may be responsible for the induction of TIMP-1 observed in this study. MMP-2 and TIMP-2 share the AP-2 promoter, and this may explain why mRNA levels of both these genes paralleled each other. TIMP-4 is of particular interest in HF because it is predominantly expressed in the heart [7]. TIMP-4 mRNA levels did not significantly change at any timepoint in this study while protein levels dropped substantially at 1 and 8 weeks post-MI. This result resembles that reported in human HF patients [13], how-

ever, it is not obvious why TIMP-4 should decrease at these specific timepoints, nor what effect decreased TIMP-4 has on MMP activity. The ratio of free MMP-1 to that bound to TIMP-1 has been reported to increase in failing human hearts [3]. Decreased TIMP binding to MMPs in HF may be due to an alteration in MMP versus TIMP localization. In vivo TIMP inhibitory activity appears to be more than just the sum of protein levels.

4.3. Conclusions

MMP/TIMP upregulation evolves over time following ischemia in the rat LV. Activation of rat interstitial collagenase (MMP-13) is predominant during scar formation. After MI wound healing upregulation of neutrophil collagenase (MMP-8), pro-MMP-13, and membrane type-1 MMP (MMP-14) protein levels occur at different timepoints out to the development of HF. Protein levels of MMPs (-2, -9, -13, and -14) increased without a corresponding increase in mRNA levels indicating post-translation processing. If these results can be extrapolated to the pathogenesis of progressive HF in humans then broad-spectrum enzyme inhibitors (as opposed to the manipulation of upstream regulators) may be the best pharmacological target for altering MMP driven LV remodeling.

References

- [1] Borg TK, Burgess ML. Holding it all together: organization and function(s) of the extracellular matrix in the heart. *Heart Failure* 1993;8:230–238.
- [2] Cleutjens JP. The role of matrix metalloproteinases in heart disease. *Cardiovasc Res* 1996;32:814–821.
- [3] Coker ML, Zellner JL, Crumbley AJ, Spinale FG. Defects in matrix metalloproteinase inhibitory stoichiometry and selective MMP induction in patients with nonischemic or ischemic dilated cardiomyopathy. *Ann NY Acad Sci* 1999;878:559–562.
- [4] Dollery CM, McEwan JR, Henney AM. Matrix metalloproteinases and cardiovascular disease. *Circ Res* 1995;77:863–868.
- [5] Fujisawa T, Hattori T, Takahashi K, Kuboki T, Yamashita A, Takigawa M. Cyclic mechanical stress induces extracellular matrix degradation in cultured chondrocytes via gene expression of matrix metalloproteinases and interleukin-1. *J Biochem (Tokyo)* 1999;125:966–975.
- [6] Fukuda Y, Ishizaki M, Kudoh S, Kitaichi M, Yamanaka N. Localization of matrix metalloproteinases-1, -2, and -9 and tissue inhibitor of metalloproteinase-2 in interstitial lung diseases. *Lab Invest* 1998;78:687–698.
- [7] Greene J, Wang M, Liu YE, Raymond LA, Rosen C, Shi YE. Molecular cloning and characterization of human tissue inhibitor of metalloproteinase 4. *J Biol Chem* 1996;271:30375–30380.
- [8] Gunja Smith Z, Morales AR, Romanelli R, Woessner Jr. JF. Remodeling of human myocardial collagen in idiopathic dilated cardiomyopathy. Role of metalloproteinases and pyridinoline cross-links [see comments]. *Am J Pathol* 1996;148:1639–1648.
- [9] Heymans S, Luttun A, Nuyens D et al. Inhibition of plasminogen activators or matrix metalloproteinases prevents cardiac rupture but impairs therapeutic angiogenesis and causes cardiac failure [see comments]. *Nat Med* 1999;5:1135–1142.
- [10] Itoh Y, Ito A, Iwata K, Tanzawa K, Mori Y, Nagase H. Plasma membrane-bound tissue inhibitor of metalloproteinases (TIMP)-2 specifically inhibits matrix metalloproteinase 2 (gelatinase A) activated on the cell surface. *J Biol Chem* 1998;273:24360–24367.
- [11] Janowska-Wieczorek A, Marquez LA, Nabholz JM et al. Growth factors and cytokines upregulate gelatinase expression in bone marrow CD34(+) cells and their transmigration through reconstituted basement membrane. *Blood* 1999;93:3379–3390.
- [12] Jugdutt BI, Joljart MJ, Khan MI. Rate of collagen deposition during healing and ventricular remodeling after myocardial infarction in rat and dog models. *Circulation* 1996;94:94–101.
- [13] Li YY, Feldman AM, Sun Y, McTiernan CF. Differential expression of tissue inhibitors of metalloproteinases in the failing human heart. *Circulation* 1998;98:1728–1734.
- [14] Li YY, McTiernan CF, Feldman AM. Proinflammatory cytokines regulate tissue inhibitors of metalloproteinases and disintegrin metalloproteinase in cardiac cells. *Cardiovasc Res* 1999;42:162–172.
- [15] McElmurray JH, Mukherjee R, New RB et al. Angiotensin-converting enzyme and matrix metalloproteinase inhibition with developing heart failure: comparative effects on left ventricular function and geometry. *J Pharmacol Exp Ther* 1999;291:799–811.
- [16] Moll UM, Youngleib GL, Rosinski KB, Quigley JP. Tumor promoter-stimulated M_r 92 000 gelatinase secreted by normal and malignant human cells: isolation and characterization of the enzyme from HT1080 tumor cells. *Cancer Res* 1990;50:6162–6170.
- [17] Nagase H, Woessner Jr. JF. Matrix metalloproteinases. *J Biol Chem* 1999;274:21491–21494.
- [18] Rohde LE, Aikawa M, Cheng GC et al. Echocardiography-derived left ventricular end-systolic regional wall stress and matrix remodeling after experimental myocardial infarction. *J Am Coll Cardiol* 1999;33:835–842.
- [19] Rohde LE, Ducharme A, Arroyo LH et al. Matrix metalloproteinase inhibition attenuates early left ventricular enlargement after experimental myocardial infarction in mice. *Circulation* 1999;99:3063–3070.
- [20] Seccia TM, Bettini E, Vulpis V et al. Extracellular matrix gene expression in the left ventricular tissue of spontaneously hypertensive rats. *Blood Press* 1999;8:57–64.
- [21] Shimizu N, Yoshiyama M, Takeuchi K et al. Doppler echocardiographic assessment and cardiac gene expression analysis of the left ventricle in myocardial infarcted rats. *Jpn Circ J* 1998;62:436–442.
- [22] Spinale FG, Coker ML, Krombach SR et al. Matrix metalloproteinase inhibition during the development of congestive heart failure: effects on left ventricular dimensions and function. *Circ Res* 1999;85:364–376.
- [23] Spinale FG, Coker ML, Thomas CV, Walker JD, Mukherjee R, Hebbard L. Time-dependent changes in matrix metalloproteinase activity and expression during the progression of congestive heart failure: relation to ventricular and myocyte function. *Circ Res* 1998;82:482–495.
- [24] Takahashi S, Barry AC, Factor SM. Collagen degradation in ischaemic rat hearts. *Biochem J* 1990;265:233–241.
- [25] Tan LB, Jalil JE, Pick R, Janicki JS, Weber KT. Cardiac myocyte necrosis induced by angiotensin II. *Circ Res* 1991;69:1185–1195.
- [26] Thomas CV, Coker ML, Zellner JL, Handy JR, Crumbley III AJ, Spinale FG. Increased matrix metalloproteinase activity and selective upregulation in LV myocardium from patients with end-stage dilated cardiomyopathy. *Circulation* 1998;97:1708–1715.
- [27] Vincenti MP, White LA, Schroen DJ, Benbow U, Brinckerhoff CE. Regulating expression of the gene for matrix metalloproteinase-1 (collagenase): mechanisms that control enzyme activity, transcription, and mRNA stability. *Crit Rev Eukaryot Gene Expr* 1996;6:391–411.
- [28] Weber KT, Sun Y, Tyagi SC, Cleutjens JP. Collagen network of the myocardium: function, structural remodeling and regulatory mechanisms. *J Mol Cell Cardiol* 1994;26:279–292.
- [29] Woessner Jr. JF. Matrix metalloproteinases and their inhibitors in connective tissue remodeling. *FASEB J* 1991;5:2145–2154.